MODELING OF HARNESS SATIN WEAVE USING FINITE ELEMENT METHOD

Yutaka Arimitsu, Masahiro Eki, Yuji Sogabe, Zhiqiang Wu
Ehime University

Keywords: *textile composites, RTM, draping, harness satin, finite element method*

Abstract

Deformation of harness satin weaves in the shaping process of resin transfer molding can be simulated using the finite element method. Inter-fiber sliding at intersections of fibers should be taken into account to perform the exact simulation of fabric shaping process. Intersections of fibers of harness satin are classified into two types, interlaced and slidable. We introduced two types of solid elements (properties of the higher yield stress for interlaced intersections and the lower yield stress for slidable). Distribution of inter-fiber sliding in the shaping process and effects of molding die could be evaluated with the proposed model. Comparing deformation between plain woven fabrics and harness satin weaves, we could numerically confirm good formability of harness satin.

1 Introduction

In the fabric shaping process of resin transfer molding (RTM), which is widely employed to produce composite shells, fabric deformation depends on the kind of fabrics (e.g. plain weave or harness satin, etc.), initial orientation of yarns and the shape of the tools. To predict properties of composites and formability of fabrics, simulation of the fabric shaping process is actually required in engineering fields.

Since the formability of harness satin fabrics is better than plain fabrics, more complicated shapes can be produced in preforming process. The formabilities of harness satin dry fabrics, laminates and prepregs were studied by Rozant et al. [1], [2] and Chang et al. [3], respectively. Shear resistance of 5-harness satin was investigated by Lomov and Verpoest [4]. Formability and angle-lock of 5-harness satin and 8-harness satin were experimentally investigated by Yu et al. [5]. Numerical approaches to solving preforming problems of woven fabrics including inter-fiber sliding were reported by Lai et al. [6] and Sidhu et al. [7], however, most research is still focused on plain woven fabrics.

The authors reported the modeling for plain woven fabrics using elastic-plastic properties of solid elements as intersection of fibers [8]. In this paper, we modify the model so it can be applied to the intersections of harness satin, which are constructed with two kinds of soft solid elements and hard cable elements. The inter-fiber sliding in the introduced model can be evaluated by elastic-plastic properties of solid elements.

Long et al. [9] identified two mechanisms of fabric deformation during the shaping process: simple shear deformation and inter-fiber sliding at the fiber crossovers. At large shear angles (up to 60-70degrees), the 'fiber lock-up' occurs. In deformation analysis of harness satin fabrics, the model includes two interactive mechanisms, since both effects of shear deformation and inter-fiber sliding of harness satin are considerably larger than plain woven fabrics.

2 Model of Harness Satin

2.1 Intersection of Fibers in Harness Satin

Since all intersections of fibers in plain woven fabrics are interlaced (see Fig.1(a)), the inter-fiber sliding is small and fabrics are apt to wrinkle in deep drawing. In the case of 5-harness satin, 20% of intersections are interlaced and other intersections are slidable (see Fig.1(b)). Consequently, the inter-fiber sliding is large and fabrics are more formable.

Since plastic deformation is related to microscopic slippage of materials, intersections of fabrics are modeled as soft solid elements reinforced with hard cable elements on upper and lower surfaces, which possess elastic-plastic properties (see Fig.2). Setting the yielding stress of solid elements I, (modeling interlaced intersections), higher than that of solid elements II, (modeling slidable intersections), microscopic deformation of satin weave can be simulated.

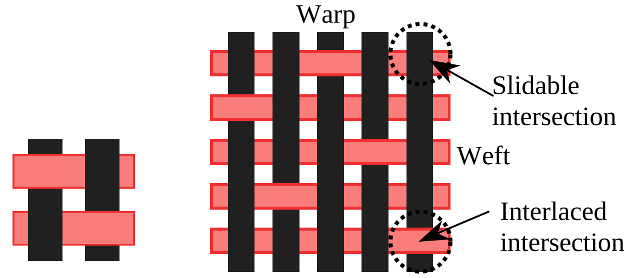

(a) Plain weave (b) 5-harness satin

Fig. 1. Woven fabric patterns

Properties of elements can be determined by the results of tensile test of fabrics and fitting them on the simulated load–strain curve. In this paper, we assume properties of elements as listed in Table 1.

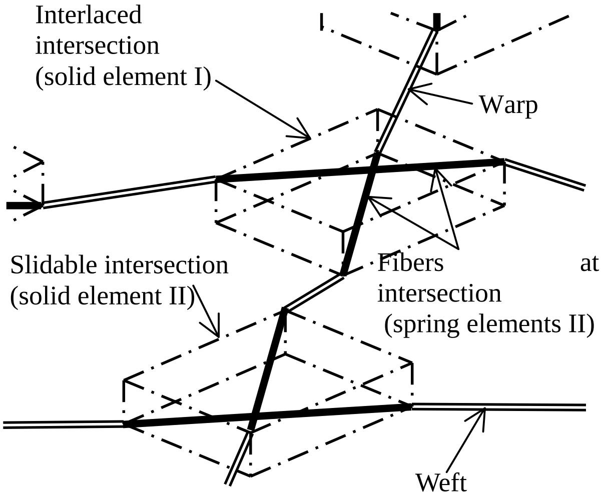

Fig. 2. Modeling of harness satin weave

Figure 3 shows the model of the intersection (details of a solid element in Fig.2) exhibiting non-linear properties of fabrics in tension. Figure 4 (a) and (b) show schematic diagrams of properties between the load P and the displacement λ. Spring elements II are correspond to the fabric properties in tension and compression, and spring elements III are related to the 'lock-up' properties of the warp and weft at intersections. The lock-up occurs over the value of a in Fig.4(b).

Table 1. Mechanical properties of elements

	Young's Modulus (MPa)	Poisson's Ratio	Spring Constant (N/mm)	Yield Stress (MPa)
Solid Element I	400	0.3	–	0.01
Solid Element II	400	0.3	–	0.1
Truss Element	4000	0.3	–	–
Non-linear Spring Element I	–	–	6930	–
Non-linear Spring Element I	–	–	7000	–

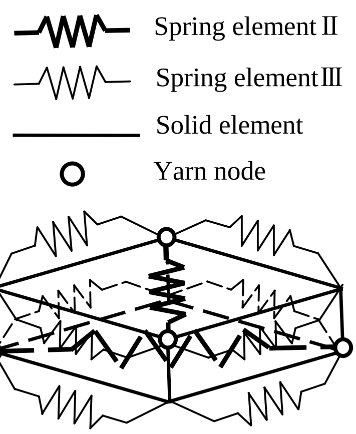

Fig. 3. Modeling of intersection of fibers

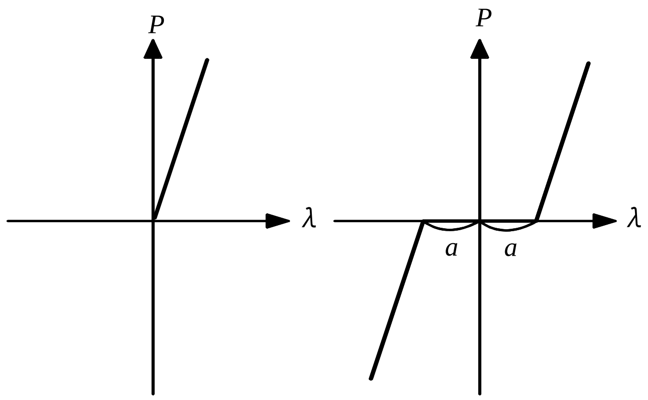

(a) Spring element II (b) Spring element III

Fig.4 Load-displacement properties of spring elements.

2.2 Definition of Inter-fiber Sliding

Inter-fiber sliding is defined as the difference between the original inter-section of undeformed fabrics and the intersection after shaping.

Let us consider the intersection modeled with a solid element which possesses four nodes of fiber segments A(x_1, y_1, z_1), B(x_2, y_2, z_2), C(x_3, y_3, z_3), D(x_4, y_4, z_4) as shown in Fig. 5. Point P in the figure (the shortest distance from B via P to D) can be regarded as the intersection of fibers.

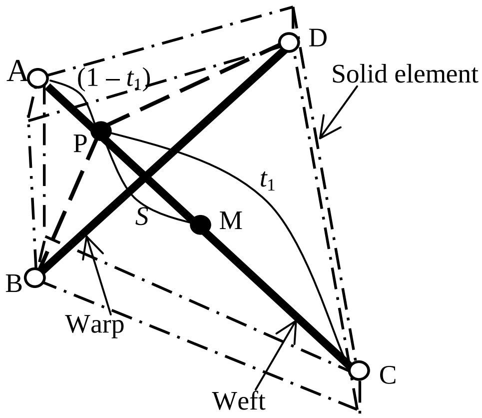

Fig. 5. Sliding at intersection of fibers.

We can get the value t_1 from coordinates of nodes A-D as follows:

(1)

The amount of inter-fiber sliding on the weft is defined as the distance from the middle point M to P. Applying similar procedure to the warp segment, we determine the amount of inter-fiber sliding on the warp. Finally, the amount of inter-fiber sliding is determined by which segment has slipped the most.

3 Numerical Results

3.1 Simulation of bias tensile test

Uniaxial tensile tests are performed to evaluate overall properties of woven fabrics, however, the evaluation of the properties of fabrics depend on measurement methods. Properties of harness satin fabrics determined using picture frame and bias experiments, which are tensile tests, were compared by Harrison et al. [10]. In the present paper, the typical ±45 degree bias tensile test is employed. After tensile deformation, three deformation zones are identified as follows (see Fig.6):

Zone I: Both warp and weft are fixed at one end. The angle between warp and weft never change during deformation, and there is little inter-fiber sliding in this zone.

Zone II: Either warp or weft is fixed at one end. The angles between warp and weft change during deformation, and there is a little inter-fiber sliding in this zone.

Zone III: This zone is free from the constrained ends. The angles between yarns change to the locking angle and the inter-fiber sliding are apt to occur.

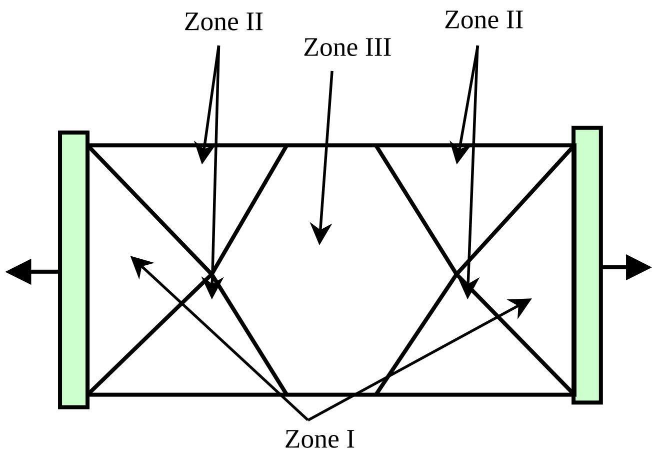

Fig. 6 Three deformation zones in tensile tests.

To evaluate mechanical properties of fabrics from element's properties using the finite element method, we simulated, as case studies, the ±45 degree bias tensile test assuming mechanical properties of elements listed in table 2.

Table 2. Mechanical properties of elements

	Case 1	Case 2	Case 3	Case 4
Young's Modulus of Solid Element I (MPa)	400	4000	400	400
Young's Modulus of Solid Element II (MPa)	400	4000	400	400
Yield Stress of Solid Element I (MPa)	0.01	0.01	0.1	0.01
Yield Stress of Solid Element II (MPa)	0.1	0.1	1	0.1
Offset *a* of Non-linear Spring Element III (mm)	±0.8	±0.8	±0.8	±0.5

Deformation profiles (tensile strain: 25%) and distribution of inter-fiber sliding of plain woven fabrics and harness satin are shown in Fig.7. In the case of plain weave, clear boundaries of zones appear and large inter-fiber sliding occurs at boundaries of each zone (see Fig.7(a)). In the case of harness satin, boundaries between zone II and III are not clear and large inter-fiber sliding occurs in the zone III, because the fabrics possesses more slidable intersections than the plain woven fabrics.

The simulated load-strain diagrams are shown in Fig.8. The locking angle in the figure, which is caused by resistance of angle change between the warp and weft, disappears in harness satin, and then the load-strain curves become flatter.

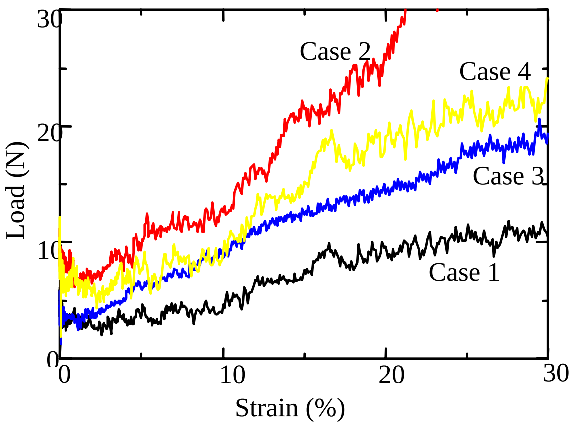

Fig.8 Load-strain diagram of harness satin fabrics.

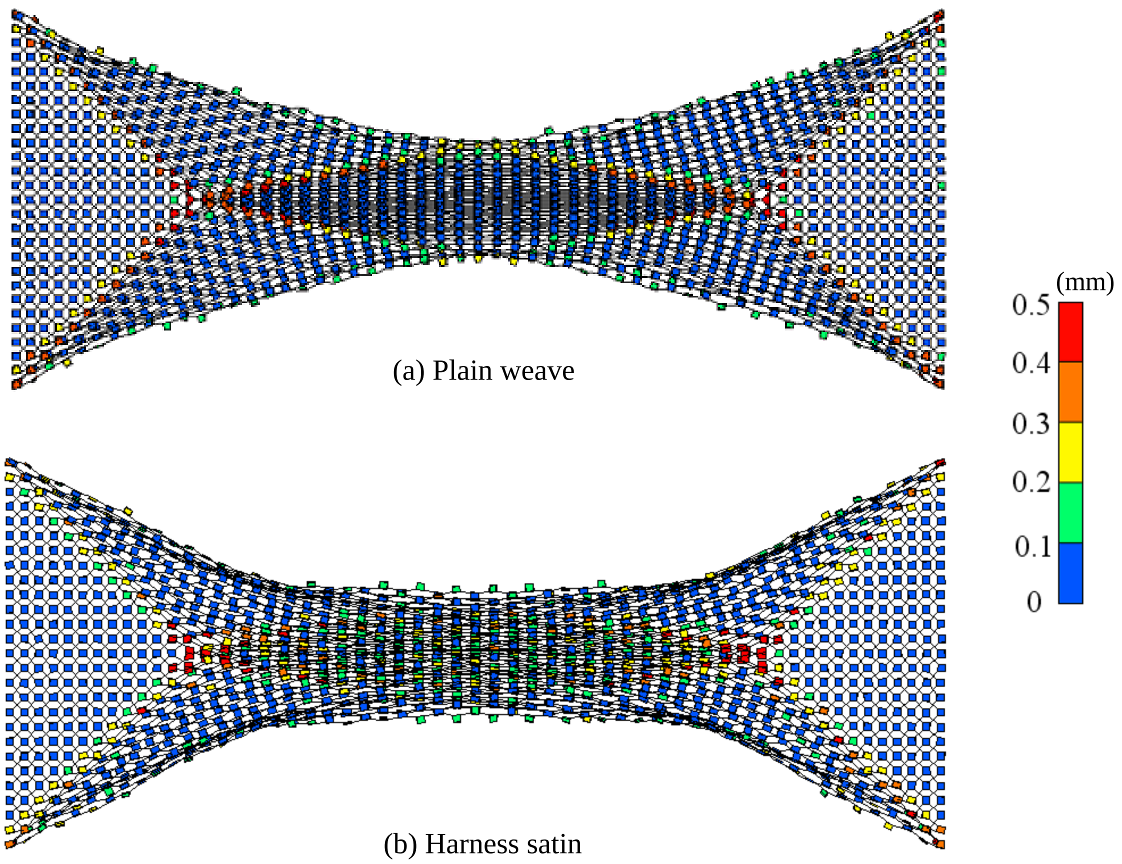

Fig.7 Distribution of inter-fiber sliding in bias tensile test.

3.2 Simulation of fabric shaping

The entire system simulated in this paper is shown in Fig. 9. Figure 10 (a) and (b), where solid elements are gradated, show the distribution of inter-fiber sliding. The amount of inter-fiber sliding in harness satin is larger than that in plain woven fabrics. The larger inter-fiber sliding appears on the side surface of cylindrical punch near the basal plane.

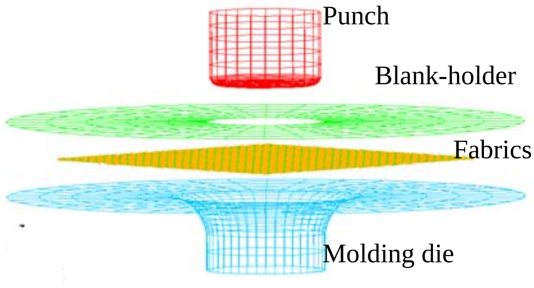

Fig. 9. Simulated system with FEM.

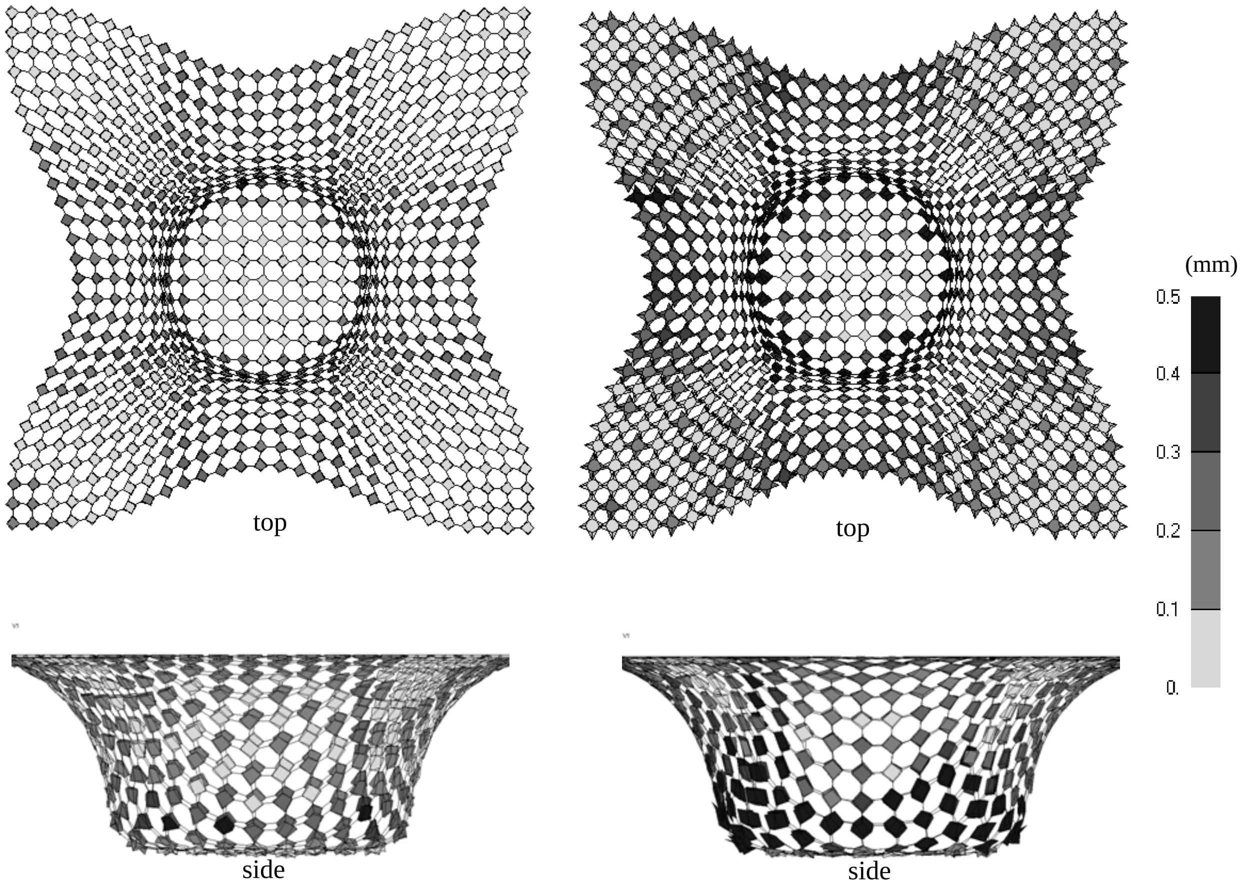

(a) Plain woven fabric (b) 5-harness stain fabric

Fig. 10. Distribution of inter-fiber sliding.

3.3 Relation between radius of molding die and inter-fiber sliding

Formability of fabrics depends on shapes of tools, for example, the radius of the molding die. To estimate the detailed dimensions of tools is one of the important purposes of simulation of fabric shaping. To show the utility of the proposed model, relations between the radius of molding die and inter-fiber sliding of harness satin fabrics are simulated. Mechanical properties of elements are employed in Table 1 and Case 1 in Table 2. In all cases, punch travel is 20mm, the punch velocity 500mm/s, static and dynamic friction coefficients are assumed to be 0.01. Inter-fiber sliding with dies of radiuses (r_2) 12mm, 14mm and 16mm are shown in Figs.11 (a), (b) and (c), respectively. The pattern of sliding distribution in harness satin fabrics is that the larger value of r_2 the smaller the sliding. There is similar tendency in plain woven fabrics [8].

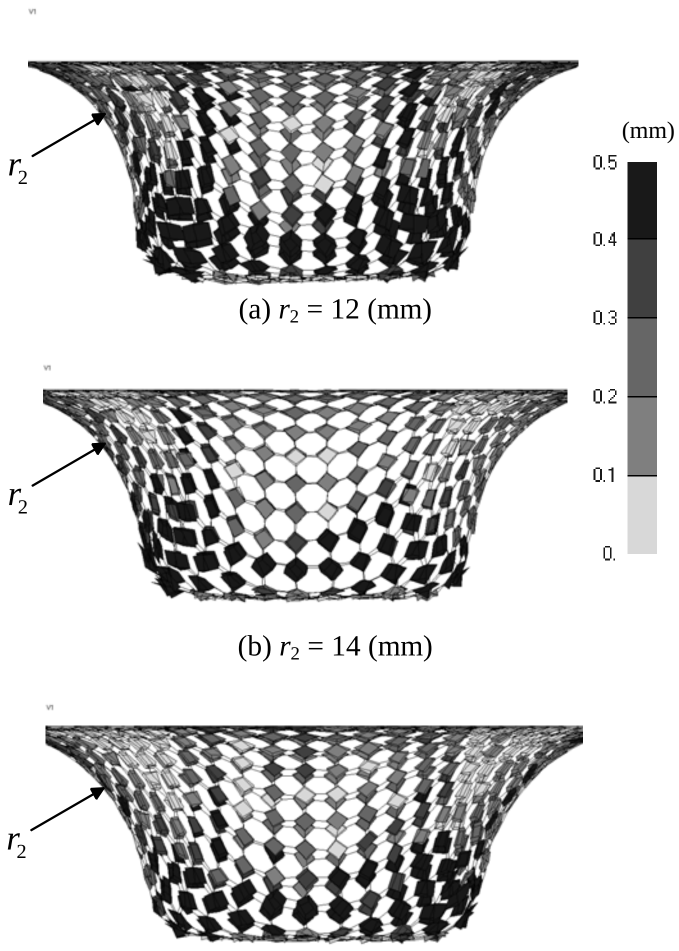

(a) r_2 = 12 (mm)

(b) r_2 = 14 (mm)

(c) r_2 =16 (mm)

Fig.11 Distribution of inter-fiber sliding.

4 Conclusions

We propose a model for harness satin fabrics using the finite element method. Assigning interlaced and slidable intersections to respective solid elements (properties of the higher yield stress for interlaced intersections and the lower yield stress for slidable), we model well-moldable satin fabrics. Mechanical properties of elements can be estimated by the bias extension test of fabrics. Using the proposed model, the distribution of inter-fiber sliding can be evaluated. We can numerically confirm that the inter-fiber sliding of harness satin is larger than plain woven fabrics.

References

[1] Rozant O., Bourban P.-E. and Manson J.-A.E. “Drapability of dry textile fabrics for stampable thermoplastic performs”. *Composites: Part A*, Vol. 31, pp1167-1177, 2000.

[2] Rozant O., Bourban P.-E. and Manson J.-A.E. “Warp-knit laminates for stampable sandwich performs”. *Composites Science and Technology* Vol. 61, pp145-156, 2001.

[3] Chang S.H., Sutcliffe M.P.F. and Sharma S.B. “Microscopic investigation of tow geometry changes in a woven prepreg material during draping and consolidation”. *Composite Science and Technolog*y, Vol. 64, pp1701-1707, 2004.

[4] Lomov S.V. and Verpoest I. “Model of shear of woven fabric and parametric description of shear resistance of glass woven reinforcements”. *Composites Science and Technology*, Vol. 66, pp919-933, 2006.

[5] Yu J.Z., Cai Z. and Ko F.K. “Formability of textile performs for composite applications. Part 1: characterization experiments”. *Composites Manufacturing*, Vol. 5, No.2, pp113-122, 1994.

[6] Lai C.L and Young W.B. “Modeling fiber slippage during the preforming process”. *Polymer Composites*, Vol. 20, No. 4, pp594-603, 1999.

[7] Sidhu R.M.J.S., Averill R.C. Riaz M. and Pourboghrat F. “Finite element analysis of textile composite preform stamping”. *Composite Structure*, Vol. 52, pp 483-497, 2001.

[8] Arimitsu Y., Ohkita M., Sogabe Y., Wu Z.Q. and Chou T.W. “Modeling of Inter-fiber Sliding in Fabric Shaping Process”. *Proceedings of 6th World Congress on Computational Mechanics*, Beijing, China, Vol. 2, CD-ROM, 2004.

[9] Long A.C., Rudd C.D., Blagdon M., Smith P. “Characterising the processing and performance of aligned reinforcements during perform manufacture”. *Composites Part A*, Vol.27, pp247-253, 1996.

[10] Harrison P., Clifford M.J. and Long A.C. "Shear characterization of viscous woven textile composites: a comparison between picture frame and bias extension experiments". *Composites Science and Technology*, Vol. 64, pp1453-1465, 2004.